ACS OMEGA

http://pubs.acs.org/journal/acsodf

Article

# CFD Analysis on the Diffusion and Accumulation Characteristics of Microleakage LPG in an Integrated Stove

Kan Jin,* Gaofan Lin, Qi Zhao, Yajing Liu, Jia Qiu, Yong Jiang, and Dongmei Huang*

Cite This: *ACS Omega* 2023, 8, 1271−1281

Read Online

ACCESS | Metrics & More | Article Recommendations

**ABSTRACT:** Gas microleakage, which results in gas diffusion and accumulation in domestic gas appliances, is the leading cause of indoor gas explosion accidents. To research the diffusion and accumulation characteristics of microleakage gas in domestic gas appliances, this study took an integrated stove as the research object and analyzed the effects of different leakage rates and leakage locations on the diffusion and accumulation characteristics of microleakage liquefied petroleum gas (LPG) in its interior using the computational fluid dynamics (CFD) numerical simulation method. The results show that microleakage LPG is characterized by a downward diffusion flow driven by gravity and the concentration inside the integrated stove cavity generally increases with the increase of leakage time; however, the spatial distribution is extremely inhomogeneous. In addition, the volume of the dangerous area rapidly changes with the continuous accumulation of microleakage LPG, occupying more than 50% of the cavity volume. Microleakage LPG diffusion and accumulation process are highly similar under different leakage rates; on the contrary, the location of the leakage source is closely related to the diffusion and accumulation characteristics. The diffusion distribution and accumulation position of microleakage LPG at different leakage locations present obvious differences. Typically, there is a concentration difference of 0.1−0.2% between the top and the bottom when the leakage source is located above the gas stove baffle and a concentration difference of 1.0−1.3% between the top and the bottom when the leakage source is located below the gas stove baffle. In addition, the difference in the leakage location has a significant impact on the time the concentration of LPG reaches the critical concentration, which indicates that the combustion and explosion risk of different leakage locations are highly related to the leakage time. The research can provide certain technical support for microleakage gas explosion accident prevention.

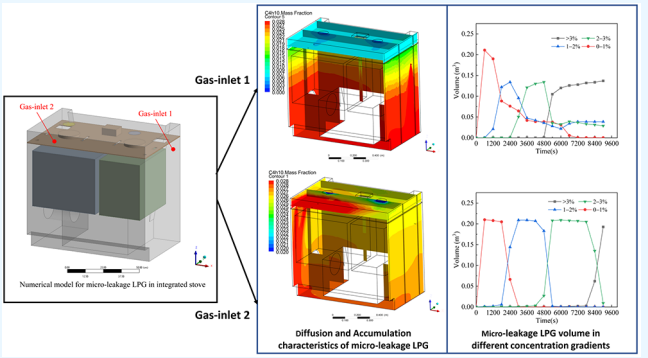


## 1. INTRODUCTION

An integrated stove is one of the domestic use modular kitchen gas-burning appliances that integrates multiple functions such as a range hood, a gas stove, and a disinfection cabinet (or oven, steam box instead).[1,2] As the people in China are continuously searching for healthier kitchens and becoming more aware of the benefits of integrated stoves, the market share of integrated stoves has grown considerably in recent years (the sales volume of integrated stoves in China from 2017 to 2021 are shown in Figure 1).[3] Moreover, the sales range of integrated stoves is gradually expanding from the Chinese market to overseas as well.[4]

Despite the success in business achieved by integrated stoves, they also cannot avoid the common problem faced by traditional domestic gas appliances, namely, the potential risk of causing an indoor gas explosion.[5,6] Figure 2 shows the ratio of indoor gas explosions to the number of total gas explosion accidents that occurred from 2017 to 2021, indicating that indoor gas explosions (mainly attributed to gas-burning appliances like integrated stoves) account for more than half of gas explosion accidents, which is also the main cause of injuries and deaths. Numerous accident investigation reports demonstrate that a major cause of indoor gas explosion accidents is the gas microleakage caused by the aging or corrosion of gas piping, which results in gas diffusion and accumulation in domestic gas appliances.[6−8]

Since the diffusion and accumulation of leakage combustible gases in confined spaces are the main reason for the accidents of indoor combustion and explosion, scholars have carried out a lot of research studies to analyze the diffusion and accumulation characteristics of leakage combustible gases in confined spaces. Some scholars used theoretical models to analyze the diffusion

**Received:** October 18, 2022
**Accepted:** December 14, 2022
**Published:** December 28, 2022

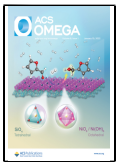

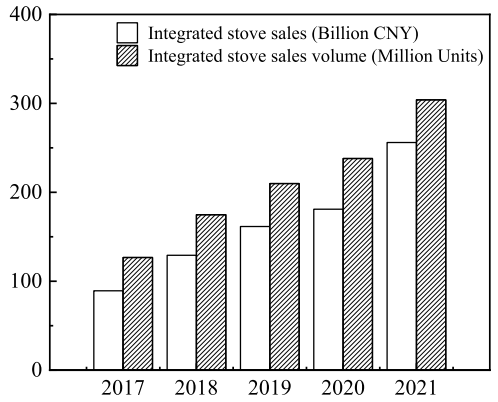


**Figure 1.** Sales of integrated stoves in China from 2017 to 2021.

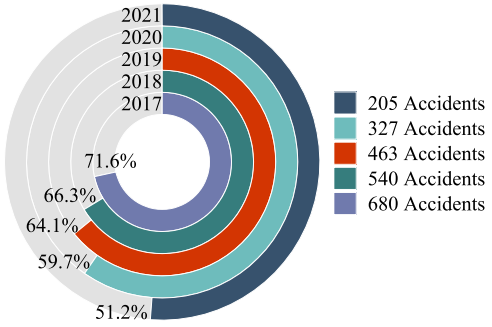


**Figure 2.** Proportion of indoor gas explosion accidents to the total gas explosion accidents (2017−2021).

and accumulation characteristics of leakage gases in confined spaces, but they did not fully characterize the short-term variability of concentrations in close proximity to the leakage source.[9−11] Whereafter, scholars carried out experiments to further study the diffusion and accumulation characteristics of leakage gas in confined spaces. Cai et al.[12] conducted relevant experiments to study the diffusion law after indoor natural gas leakage and the hazards after an explosion and determined the distribution law of indoor natural gas volume fraction under different leakage conditions, as well as the propagation laws of flames and shock waves in an explosion. Brzezińska et al.[13] conducted a series of experiments to study the dispersion distribution of leakage LPG in a confined garage, showing that under unventilated conditions, leakage LPG can accumulate on the floor of a confined garage for a prolonged time, creating a high explosion hazard.

As CFD technology has become much more mature in recent years, its advantages, such as it is suitable for research studies with complex physical models (for example, gas leakage and diffusion in small spaces with many obstacles) and can easily control the effect of each individual variable on the results, have left a deep impression on scholars. This makes the CFD technology very popular in current research, and several studies have been conducted using CFD to model gas leakage and diffusion in confined spaces.[14−18] Guo[19] used CFD software to study the gas diffusion phenomenon after indoor gas leakage under different influencing factors and analyzed in detail the diffusion process of gas in various cases, the change in the volume of the combustible area, and the consequences of combustion and explosion. Zhang et al.[20] investigated the changes in gas concentration following continuous diffusion of indoor gas leakage during different seasons by CFD software, obtained the distribution regularity of indoor gas when it reached a steady state, and examined the influence of weather and ventilation conditions on gas distribution. Wang[21] conducted an in-depth study and comparison of CFD diffusion models after kitchen leakage, simulated the diffusion state after indoor gas leakage using the modified model, and determined the concentration field distribution law in the indoor diffusion process at different times and pressure conditions after gas leakage. Li et al.[22] used CFD turbulence modeling with the correction of buoyancy effects, obtaining the diffusion characteristics of different positions after indoor gas leakage under the influence of wind speed and the component transport model. The results showed that different hazardous areas were formed after the gas leaked out and diffused at different locations. Tulach et al.[23] used CFD models to investigate the way (velocities and directions) of distribution of natural gas leaking out of predefined leakage to the confined space, and the areas were defined where local hazardous concentrations were formed. The results improved the understanding of the spreading and distribution of a mixture of gaseous fuels in confined spaces.

Although many studies have been conducted on gas leakage and dispersion laws in confined spaces, the size of numerical models built is usually on the scale of a room or even bigger (ranges from several ten cubic meters to one hundred cubic meters) and the gas leakage is also set to quite high rates (ranges from several hundred liters per hour to several thousand liters per hour) so that typical results can be achieved. In stark contrast, corresponding studies on the diffusion and accumulation characteristics of microleakage gas in really small confined spaces like an integrated stove are seriously lacking. The combustion and explosion risk analysis of microleakage gas in confined spaces is also inadequate.

In this article, through the disassembling and measuring of an integrated stove, the effects of different leakage rates and locations on the diffusion and accumulation characteristics of microleakage LPG in an integrated stove were investigated using CFD simulations, and the diffusion and accumulation characteristics of microleakage LPG over time were revealed. The result of the research can provide some references for the study of microleakage gas in domestic gas appliances and the prevention of combustion and explosion accidents in integrated stoves.

## 2. CFD NUMERICAL SIMULATIONS

**2.1. CFD Modeling.** *2.1.1. Governing Equations.* CFD is a discipline consisting of fluid mechanics, mathematics, and computer science, which is based on fluid mechanics and numerical computational methods,[24,25] starting from the basic conservation equations (mass, momentum, energy conservation equations, etc.) and performing numerical calculations under the constraints of certain initial and boundary conditions to achieve the simulation of the specified flow field.[26,27] The governing equations involved in the simulation of gas leakage from the integrated stove are as follows:

(1) The continuity equation (mass conservation):

$$\frac{\partial \rho}{\partial t} + \frac{\partial}{\partial x_j}(\rho u_j) = 0 \quad (1)$$

where $\rho$ is the gas density, $x$ is the coordinate, $u$ is the velocity vector, and $t$ is the time.

(2) The Navier−Stokes equation:


https://doi.org/10.1021/acsomega.2c06715
ACS Omega 2023, 8, 1271−1281

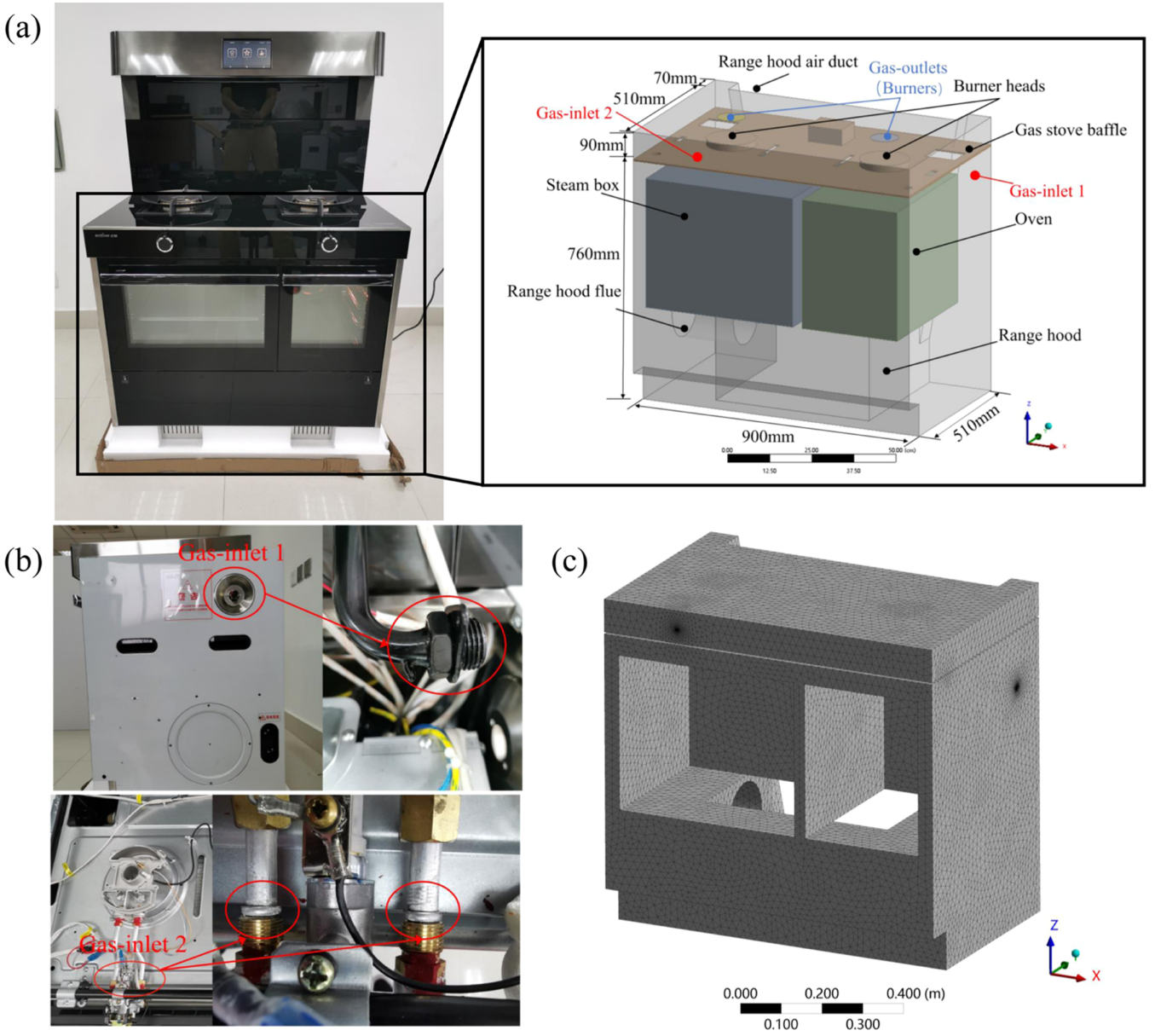


**Figure 3.** Numerical model and meshing for the study. (a) Numerical model for CFD simulations of microleakage LPG in the integrated stove. (b) The realistic locations and situations of the leakage sources in the model. (c) The meshing of the CFD model (the photographs were taken by the author, Kan Jin).

$$\frac{\partial}{\partial t}(\rho u_i) + \frac{\partial}{\partial x_j}(\rho u_i u_j) = -\frac{\partial p}{\partial x_i} + \frac{\partial}{\partial x_j}\left[(\mu + \mu_t)\left(\frac{\partial u_j}{\partial x_i} + \frac{\partial u_i}{\partial x_j}\right)\right] \quad (2)$$

where $\rho$ is the turbulent available pressure, $\mu$ is the laminar viscosity coefficient, $\mu_t$ is the turbulent viscosity coefficient, which is given as $\rho C_\mu k^2/\varepsilon$, $k$ is the turbulent kinetic energy, $\varepsilon$ is the turbulent dissipation rate, and $C_\mu$ is 0.009.

(3) The component mass conservation equation:

$$\frac{\partial(\rho c_s)}{\partial t} + \mathrm{div}(\rho u c_s) = \mathrm{div}(D_s\ \mathrm{grad}(\rho c_s)) + S_s \quad (3)$$

where $\rho$ is the volume concentration of fraction $s$, $\rho c_s$ is the mass concentration of the component, $D_s$ is the diffusion coefficient of the component, and $S_s$ is the mass of the component produced by the chemical reaction per unit volume in time within the system, i.e., productivity.

*2.1.2. Numerical Modeling and Meshing.* By disassembling and measuring the integrated stove, its internal structure, as well as the dimension parameters, is obtained, and with some certain simplifications for the internal flow channel space, a numerical model for the simulation of microleakage gas in the integrated stove is developed (as shown in Figure 3a). The internal space within the integrated stove can be generally separated into two cavities by the gas stove baffle, and the two cavities are not completely isolated from each other but connected through holes in the baffle to create an overall gas flow space. Usually, the lower cavity is equipped with a steamer, an oven, and a range hood, while the upper cavity is equipped with a gas stove and has



https://doi.org/10.1021/acsomega.2c06715
ACS Omega 2023, 8, 1271−1281

Table 1. Basic Physical Parameters of the Three Gases

| gas type | gaseous density (kg/m$^3$) | molecular weight | kinematic viscosity (m$^2$/s) | thermal conductivity (W/(m·K)) | diffusion coefficient (cm$^2$/s) | explosion limit (%) |
|---|---|---|---|---|---|---|
| LPG | 2.35 | 44.13−57.99 (56.08) | $3.56 \times 10^{-6}$ | 0.0174 | 0.121 | 1.5−9.5 |
| propane | 1.83 | 44.10 | $4.54 \times 10^{-6}$ | 0.0183 | 0.114 | 2.1−9.5 |
| butane | 2.48 | 58.12 | $3.07 \times 10^{-6}$ | 0.0163 | 0.103 | 1.9−8.5 |

two outlets (the actual burners of the gas stove) connected to the atmosphere.

To study the diffusion and accumulation characteristics of microleakage LPG, two sources of leakage are placed in the cavity of the integrated stove (named gas-inlet 1 and gas-inlet 2). Of which, leakage source 1 (gas-inlet 1) is placed at the threaded joint of the gas piping below the gas stove baffle in the lower cavity, and leakage source 2 (gas-inlet 2) is placed at the joint of the ejector above the gas stove baffle in the upper cavity (as shown in Figure 3b). The abovementioned locations serve as the joints of the gas piping, where existing rubber sealing rings may leak after long-term use due to aging; therefore, these locations are at high risk of leakage.[28,29] Moreover, in China, some illegal LPG stations would adulterate dimethyl ether into LPG for profiteering, which is corrosive to rubber sealing materials and accelerates the aging of rubber sealing rings, thus finally aggravating the hidden danger of gas leakage.[30−32] In addition, the placement of the leakage sources below and above the baffle of the gas stove also facilitates the study of the effect of the location of the leakage source on the diffusion and accumulation of microleakage LPG.

During the simulation process, it is important to verify that the divided mesh is independent of the mesh size to remove the impact of the mesh size on the simulation results.[33] After adjusting the mesh size in several simulation tests, the best quality mesh was obtained for this simulation using a tetrahedral grid. Using a grid cell size of 1.98 mm, local encryption was performed at the source of leakage with high turbulence. The maximum skewness value is 0.79864, the average value is 0.23063, and the number of grid cells is 388643. The mesh division results are shown in Figure 3c.

**2.2. Boundary Conditions and Solution.** ANSYS Fluent software was used to perform CFD simulations in this study. The simulations were conducted using Fluent's pressure solver and the *k*-epsilon gas flow model. Xing et al.[34] demonstrated that the standard *k*-epsilon model performed better in simulations of heavy gas diffusion, and the simulation results were validated by experimental results. The diffusion process of the gas was modeled by Fluent's species transport model.[35] Due to the lack of LPG-related parameters in the Fluent gas database, and the fact that LPG consists primarily of propane and butane gas as its main components, Liang et al.[36] used a mixture of 47% propane and 53% butane instead of LPG. We compared the physical characteristics (gaseous density, molecular weight, and explosion limit) and transport properties (kinematic viscosity, thermal conductivity, and diffusion coefficient) of both gases and LPG (as shown in Table 1), and it should be noted that the light hydrocarbon components of LPG improve its diffusion coefficient. To easily analyze the diffusion process of microleakage LPG, finally, butane gas, which is closest to LPG in physical characteristics and transport properties, was chosen as the leakage source gas in the simulation.

The leakage rates of LPG used in simulations were determined based on the related regulations of GB 17905−2008 (Safety management regulation of gas-burning appliances for domestic use),[37] which states that "under 4.2 kPa air pressure, the leakage amount should be less than 0.07 L/h". Thus, four simulation scenarios were set up (four scenarios with microleakage gas rates set at 1, 2, 5, and 10 times the standard leakage rate of 0.07 L/h, as shown in Table 2) to analyze the characteristics of gas diffusion and accumulation within the integrated stove at different leakage intensities. Moreover, due to the limitation of the software setup, the microleakage gas rates were substituted into the simulation as mass flow rates. For each scenario, leakage was simulated continuously at 300 K for 150 min.

Table 2. Gas Leakage Scenario Setup in CFD Simulations

| simulation scenarios | locations of leakage | leakage rates (L/h) | corresponding mass flow rates (kg/s) |
|---|---|---|---|
| 1 | leakage source 1 | 0.07 | $4.822 \times 10^{-8}$ |
| 2 | | 0.14 | $9.644 \times 10^{-8}$ |
| 3 | | 0.35 | $2.411 \times 10^{-7}$ |
| 4 | | 0.70 | $4.822 \times 10^{-7}$ |
| 5 | leakage source 2 | 0.07 | $4.822 \times 10^{-8}$ |
| 6 | | 0.14 | $9.644 \times 10^{-8}$ |
| 7 | | 0.35 | $2.411 \times 10^{-7}$ |
| 8 | | 0.70 | $4.822 \times 10^{-7}$ |

## 3. RESULT ANALYSES

**3.1. Diffusion and Accumulation Characteristics of Microleakage LPG over Time.** *3.1.1. Diffusion Flow Characteristics of Microleakage LPG.* We chose scenarios 1 (corresponding to leakage from leakage source 1) and 5 (corresponding to leakage from leakage source 2) as typical scenarios to analyze the diffusion characteristics of microleakage LPG in the integrated stove. To show the migration characteristics of microleakage LPG more intuitively, referring to the explosion limit concentration of LPG (1.5−9.5%) and the density of butane gas (2.48 kg/m$^3$), a mass fraction of 2.84% was derived from the corresponding volume fraction of the lower explosive limit of 1.5%. Considering a certain affluence coefficient, the isosurface of the gas mass fraction = 3% (blue part of the figure) was selected as the characteristic parameter (critical concentration condition with the risk of ignition and explosion) for analyzing the diffusion flow characteristics of microleakage LPG under the influence of gravity and at a leakage rate of 0.07 L/h.

Figure 4 shows the diffusion flow characteristics of LPG under simulated scenario 1 conditions. According to the results, the initial momentum in the microleakage process was insufficient after the LPG leaked from leakage source 1, so it was affected by the molecular thermal motion[38] to diffuse from the leakage source to the interior of the cavity. Because LPG has a density 1.686 times higher than air, it slowly sank along the wall driven by gravity in the diffusion process. As the leakage time and the amount of leakage LPG increased, the LPG still sank along the wall, but its flow range continued to increase and the rate of sinking accelerated. About 80 min after the leakage, the flow


https://doi.org/10.1021/acsomega.2c06715
ACS Omega 2023, 8, 1271−1281

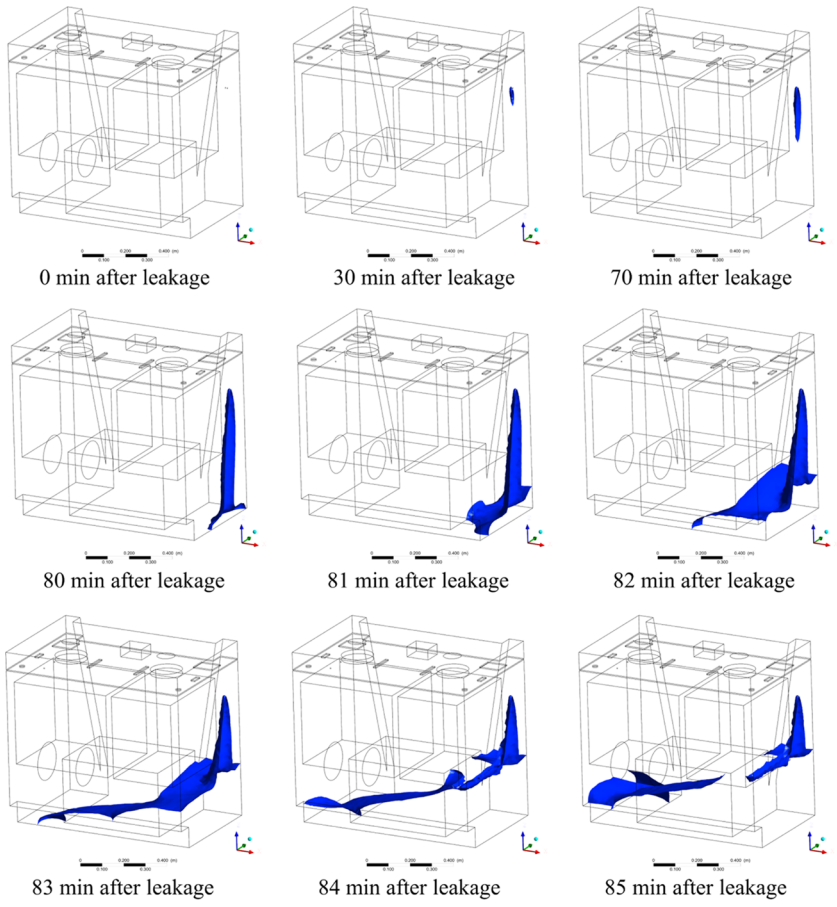


**Figure 4.** Isosurface distribution at different moments after LPG leakage (simulation scenario 1, in the blue part of the graph, gas mass fraction = 3%).

boundary of the leakage LPG reached the junction with the integrated stove cavity bottom, and by blocking the wall, the diffusion direction changed, gradually downward diffused to the cavity bottom, and rapidly accumulated there within minutes; approximately 85 min after the leakage, a large amount of LPG accumulated at the cavity bottom, and the diffused LPG exhibited accumulation characteristics in the cavity bottom.

On analyzing the diffusion flow characteristics of LPG, it was also found that after 80 min of leakage and diffusion, the mass fraction of the isosurface was rapidly changed within several minutes. According to Figure 6a, the volume of $C_4H_{10}$ with a mass fraction above 3% increased from $8.16 \times 10^{-4}$ to $1.05 \times 10^{-1}$ $m^3$ after 90 min of leakage, which occupied about 50% of the whole cavity volume. This phenomenon can be interpreted as that with the continuous leaking of LPG, the leakage gas diffused to various parts of the cavity (although the mass fraction in most areas was less than 3%), and after 80 min of leakage/diffusion, the mass fraction of LPG contained in the bottom region of the cavity was actually close to 3% in many locations (as shown in Figure 6), resulting in the accumulation area where the LPG mass fraction exceeding 3% expanded rapidly within a short period.

Figure 5 shows the diffusion flow characteristics of LPG under simulated scenario 5 conditions. According to the results, the LPG leaked from leakage source 2 downward diffused driven by gravity during the diffusion process. When the LPG sank to the baffle, it began to flow around the location below the projection of the leakage point, resulting in an inverted funnel-shaped flow pattern. With increasing leakage time and leakage amount, the flow range of gas continued to increase until it encountered the boundary following the occurrence of the state of motion. After 120 min, the flow boundary of the leakage LPG reached the junction between the upper and lower cavities of the integrated stove; then, a portion of the LPG sank and flowed through the holes in the gas stove baffle toward the lower cavity of the integrated stove, where the steamer, oven, and range hood were installed, while the remainder of the LPG that was not obstructed in the direction of movement continued to flow in a disc shape in all directions. Approximately 136 min after leakage, the sinking leakage LPG reached the integrated stove cavity bottom and gradually accumulated there. The diffused LPG exhibited accumulation characteristics in the cavity bottom and on the gas stove baffle, which was different from the accumulation pattern of scenario 1 conditions. According to Figure 6b, the volume of $C_4H_{10}$ with a mass fraction above 3% increased from $2.73 \times 10^{-3}$ to $6.21 \times 10^{-2}$ $m^3$ after 140 min of leakage, which occupied about 30% of the whole cavity volume. Then, 150 min after leakage, the volume increased to $1.37 \times 10^{-1}$ $m^3$, which occupied about 65% of the whole cavity volume.

*3.1.2. Spatial Distribution Characteristics of Microleakage LPG.* To more detailedly analyze the spatial distribution characteristics of the microleakage LPG over leakage time, the distribution characteristics of LPG inside the integrated stove after scenario 1 leakage (as shown in Figures 7 and 9a) and the distribution characteristics of LPG inside the integrated stove after scenario 5 leakage (as shown in Figures 8 and 9b) were taken as examples. The analysis result indicated that regardless of leakage source location, as the LPG has the characteristics of



https://doi.org/10.1021/acsomega.2c06715
ACS Omega 2023, 8, 1271−1281

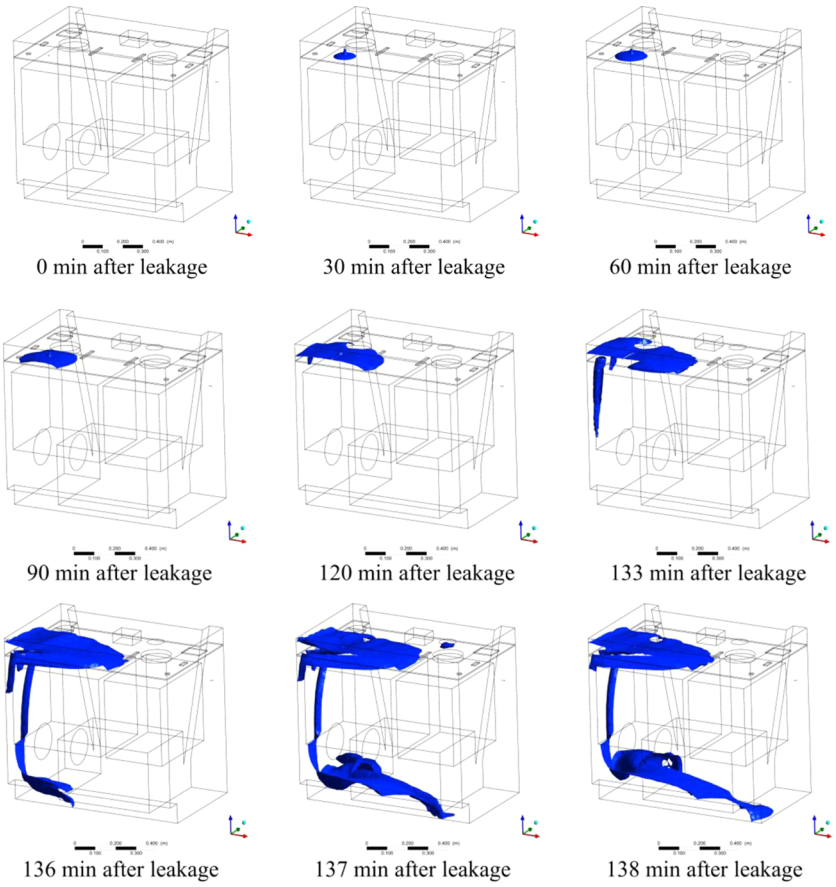


**Figure 5.** Isosurface distribution at different moments after LPG leakage (simulation scenario 5, in the blue part of the graph, gas mass fraction = 3%).

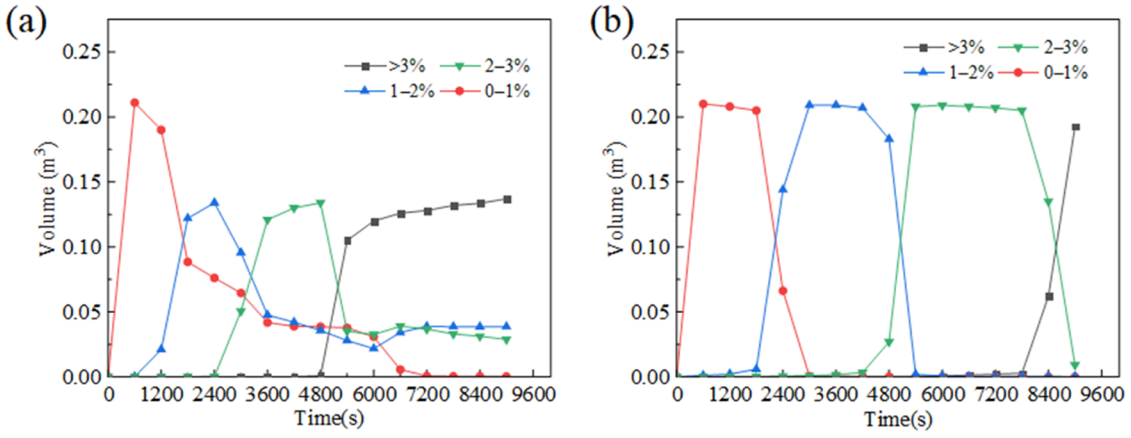


**Figure 6.** $C_4H_{10}$ volume in different concentration gradients: (a) scenario 1 and (b) scenario 5.

high density and small diffusion coefficient, the concentration of LPG inside the integrated stove cavity generally increased with increased leakage time; however, the spatial distribution was extremely inhomogeneous.

In general, the leaked LPG from leakage source 1 mainly accumulated in the bottom region of the integrated stove cavity, whereas the leaked LPG from leakage source 2 not only accumulated in the cavity bottom but also accumulated in large quantities on the gas stove baffle, as indicated in Section 3.1.1. On the same longitudinal section, the concentration generally decreases with increasing height (except for the baffle). Typically, the concentration of LPG at the bottom of scenario 1 is approximately 1.0−1.3% higher than that at the top, and that at the bottom of scenario 5 is approximately 0.1−0.2% higher than that at the top; on the same cross section, the closer the location to the leakage source, the higher the concentration of accumulated LPG.

**3.2. Effect of the Leakage Rate on the Diffusion Characteristics of LPG.** To monitor the concentration variation of LPG upper at different leakage moments, monitoring points were established at the four points where the upper and lower cavity walls intersect with the longitudinal section of the leakage source based on the different locations of leakage (as shown in Figure 10), which could better reflect the diffusion and accumulation characteristics of microleakage gas, and the flow variation characteristics under the condition that



https://doi.org/10.1021/acsomega.2c06715
ACS Omega 2023, 8, 1271−1281

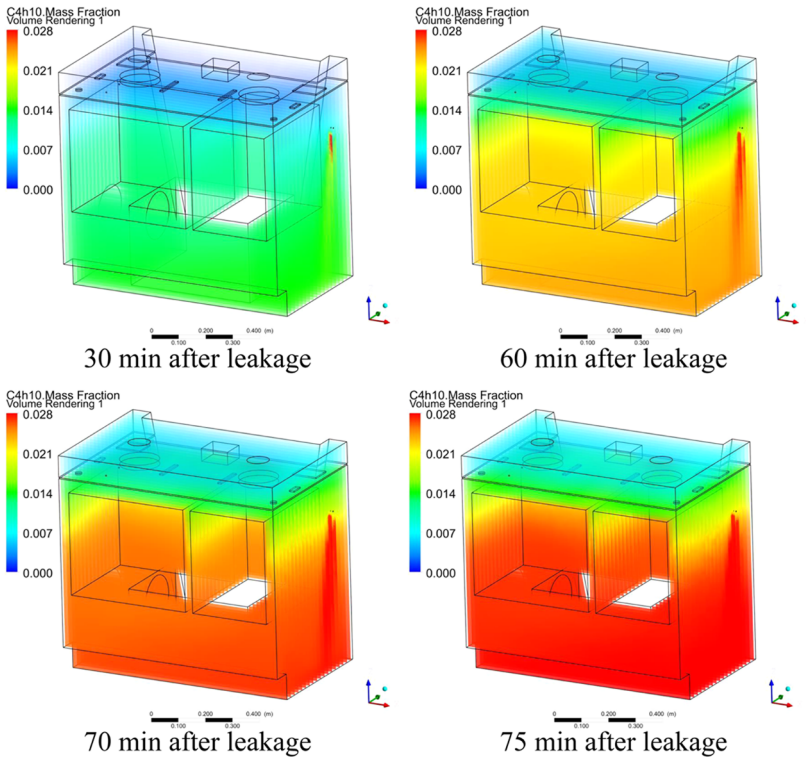


**Figure 7.** Distribution characteristics of LPG after different leakage times (scenario 1).

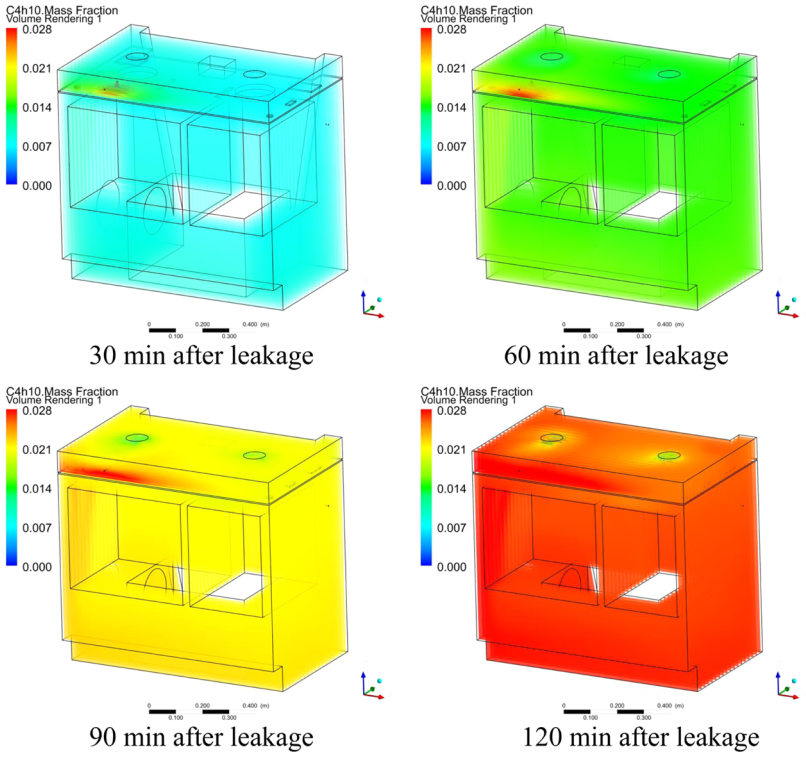


**Figure 8.** Distribution characteristics of LPG after different leakage times (scenario 5).

the diffusion process was obstructed, so that the diffusion and accumulation characteristics of microleakage LPG in the upper and lower cavities under different leakage sources conditions were able to be studied.

To analyze the relationship between the diffusion characteristics of microleakage LPG in the integrated stove and the gas leakage rate, the $C_4H_{10}$ mass fraction curve charts (as shown in Figure 11) were extracted from Figure 10 at monitoring points 1 and 2 of leakage source 1 and at monitoring points 2 and 3 of leakage source 2 at the end of simulations under simulation scenarios 1 to 8. The results show that the concentration of $C_4H_{10}$ increased faster closer to the leakage source under the



https://doi.org/10.1021/acsomega.2c06715
ACS Omega 2023, 8, 1271−1281

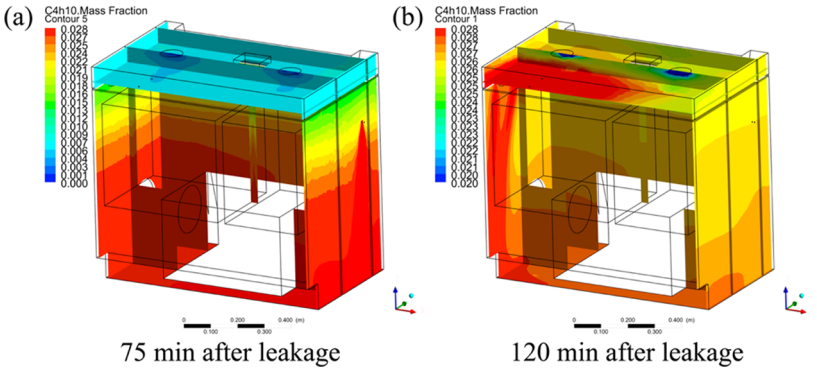


**Figure 9.** LPG mass fraction distribution cloud atlas: (a) scenario 1 and (b) scenario 5.

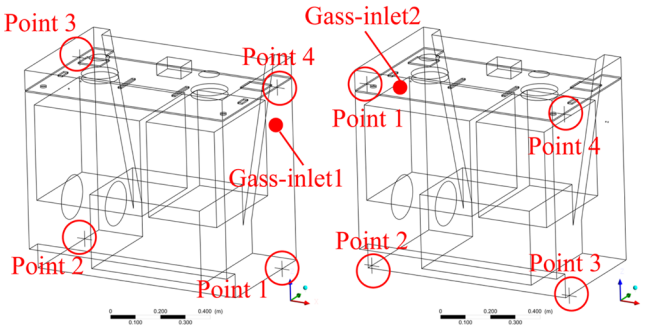


**Figure 10.** Layout drawing showing the LPG concentration monitoring points.

same diffusion characteristics as at the initial stage of leakage, and at the same monitoring point, the trend of $C_4H_{10}$ concentration changed faster as the leakage rate increased, but as the leakage continued, this trend of change slowed down, and the simulation gradually tended to the steady state. As a result, the concentration of LPG at each point was similar under different leakage rates of the same leakage source. A general observation is that the concentration curves of each monitoring point in different scenarios exhibit similar patterns and that the leakage rate at the initial stage of leakage influences the diffusion concentration of microleakage LPG in the integrated stove. LPG concentration increases as the leakage rate increases, and as it gets closer to the leakage source, it increases further.

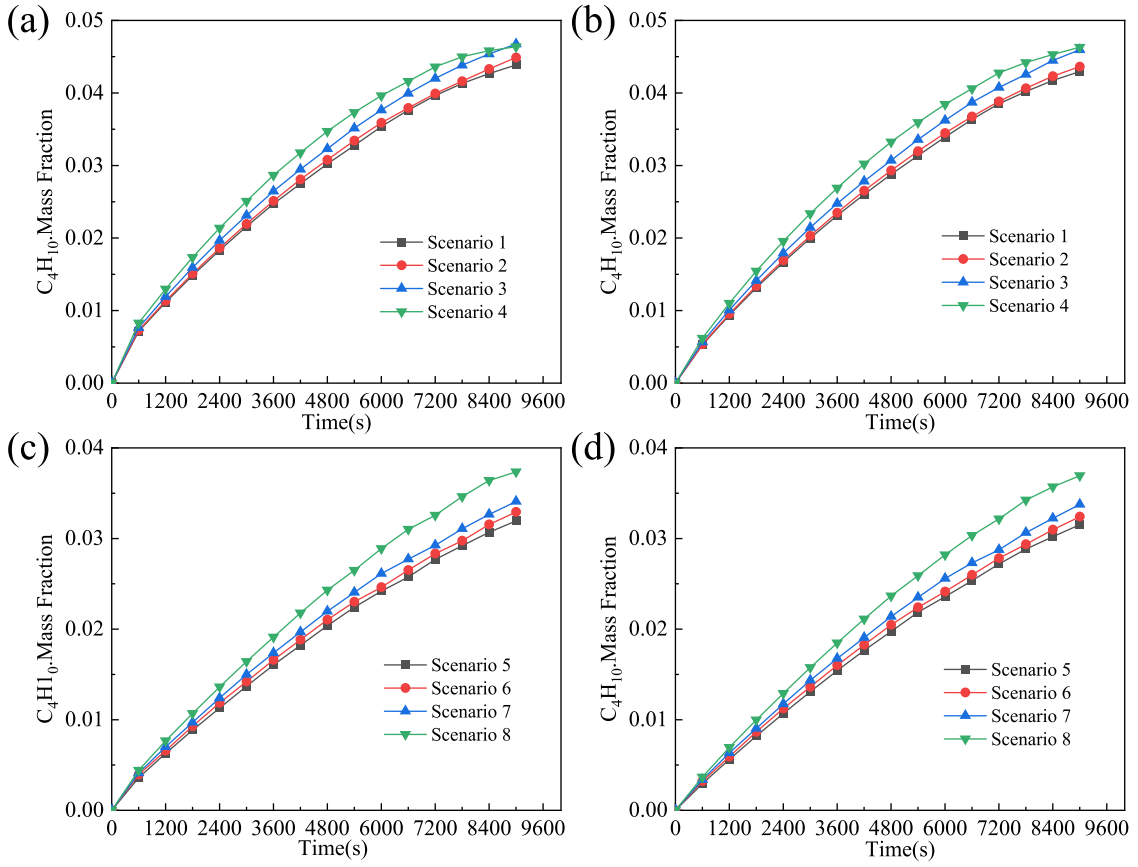


**Figure 11.** Mass fraction variation of $C_4H_{10}$ with time for different scenarios. (a) Leakage source 1: point 1; (b) leakage source 1: point 2; (c) leakage source 2: point 2; and (d) leakage source 2: point 3.



https://doi.org/10.1021/acsomega.2c06715
ACS Omega 2023, 8, 1271−1281

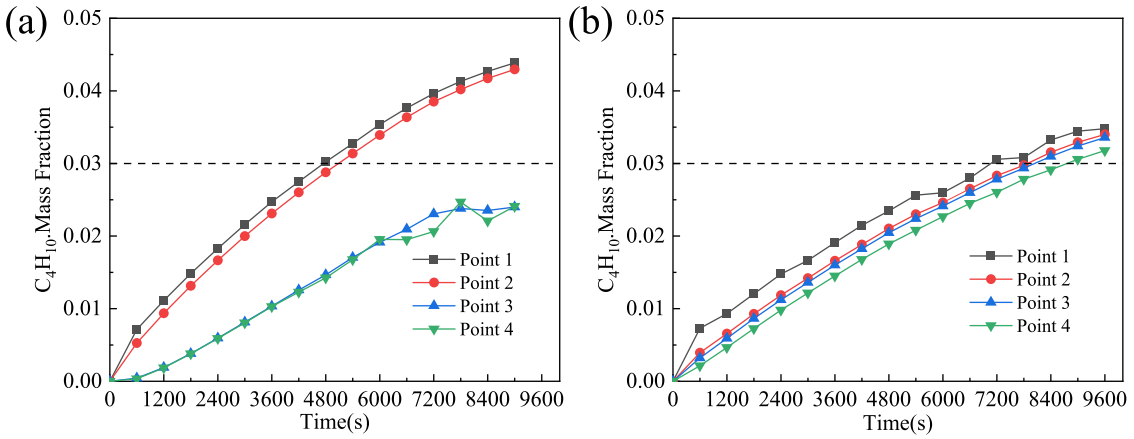


**Figure 12.** Relationship between the mass fraction of $C_4H_{10}$ and leakage time under different leak locations: (a) scenario 1 and (b) scenario 5.

In spite of the fact that the initial leakage rate has a limited impact on the distribution of LPG inside the integrated stove, the larger the leakage rate corresponding to the leakage from different sources, the faster the leakage LPG accumulates in its accumulation area and the shorter the time for the critical concentration to be reached. However, during the continuous leakage, LPG continually dilutes with the surrounding air as it diffuses downward and eventually reaches a steady state as a result of diffusion and leakage, reaching relative equilibrium.[39,40] During the leakage process, LPG with different leakage rates diffuses and accumulates in the integrated stove with the same diffusion characteristics, although the faster leakage rate can accelerate the time to reach the relative equilibrium state, but ultimately, the distribution characteristics of leakage LPG in the integrated stove are consistent. In the simulation scenarios set up in this study, when the leakage rate is 0.7 L/h, the concentration of LPG reaches the relative equilibrium earlier compared to 0.07 L/h. However, regardless of whether the LPG leakage rate is 0.07 L/h or 0.70 L/h, the diffusion and accumulation characteristics of microleakage gas are independent of the leakage rate.

**3.3. Influence of Leakage Source Location on LPG Accumulation.** According to the conclusions of Section 3.2, monitoring points 1, 2, 3, and 4 at leakage source 1 and leakage source 2 in Figure 10 were selected for plotting the $C_4H_{10}$ mass fraction curve with time at the end of the simulation in scenarios 1 and 5 (as shown in Figure 12). The analysis reveals that the diffusion and accumulation characteristics of LPG inside the integrated stove are closely related to the location of the leakage source (although they are not related to the leakage rate). For leakage source 1, the LPG concentration obtained inside the integrated stove was always higher than that of leakage source 2 under the same simulation setting, which means that the LPG concentration at the same location point 2 was always higher for leakage source 1 than that for leakage source 2. This phenomenon can be explained as follows: since leakage source 2 is located close to the top opening, some of the leakage LPG can easily escape from the top opening of the integrated stove cavity; moreover, there is a gas stove baffle between leakage source 2 and the lower cavity of the integrated stove, which also has a blocking effect on the downward diffusion of LPG. In contrast, since leakage source 1 is located below the gas stove baffle in the lower cavity, the leakage LPG can diffuse downward without blockage from the baffle. Additionally, leakage source 1 is far away from the top opening of the integrated stove cavity, which largely weakens the leakage effect of LPG and increases the concentration of LPG inside the integrated stove cavity. As a result, compared to the situation when the leakage source is located above the gas stove baffle, when the leakage source is located below the gas stove baffle, the concentration of LPG accumulated in the integrated stove increases faster, which means that it can reach the critical concentration of explosion earlier. From the simulation, it takes approximately 4500 s for leakage source 1 to reach the critical concentration of explosion in the cavity bottom but takes approximately 7200 s for leakage source 2 to reach the same critical concentration of explosion on the gas stove baffle.

Moreover, according to the comparison of the LPG concentration at each monitoring point, it was found that under scenario 1, the concentration at monitoring points 1 and 2 in the lower cavity reached critical explosion concentration relatively sooner, whereas the concentration at monitoring points 3 and 4 in the upper cavity never reached the critical explosion concentration as the leakage continued; under scenario 2, the concentration at the four monitoring points reached critical explosion concentration one after another as the leakage continued. By combining the microleakage LPG diffusion and accumulation characteristics described in Section 3.1, it can be concluded that if there exists a microleakage source in the lower cavity, the cavity bottom becomes the potential site for ignition and explosion, while if there exists a microleakage source in the upper cavity, then the entire cavity becomes the site for ignition and explosion.

## 4. DISCUSSION

Through the comprehensive study on the influence of various factors on the diffusion and accumulation characteristics of microleakage LPG in the integrated stove, the result indicates that although the different leakage rates can affect the concentration of LPG in the integrated stove, the diffusion and accumulation process of LPG under various leakage rates are highly similar, which means that the faster leakage rate can only accelerate the time to reach the critical concentration of explosion but can hardly change the LPG distribution characteristics in the integrated stove. In contrast, the location of the leakage source is closely related to the diffusion and accumulation characteristics of the microleakage LPG; when the leakage source is located below the gas stove baffle in the lower cavity, the leakage LPG mainly diffuses and accumulates in the cavity bottom, making the bottom of the cavity a potential site


https://doi.org/10.1021/acsomega.2c06715
ACS Omega 2023, 8, 1271−1281

for combustion and explosion, and when the leakage source is located above the gas stove baffle in the upper cavity, the leakage LPG not only accumulates in the cavity bottom but also accumulates on the gas stove baffle, making the entire cavity a potential site for combustion and explosion. Additionally, when the leakage occurs in the lower cavity of the integrated stove, the concentration of LPG accumulated in the stove can reach the critical concentration of explosion faster than the leakage occurring in the upper cavity.

Based on the above analyses, the risk of ignition and explosion caused by microleakage LPG from an integrated stove can be analyzed. Due to the fact that two main ignition sources were identified when disassembling the integrated stove, namely, the naked fire generated by the gas stove burner and the sparks (may) generated by the electrical appliances in the lower cavity, then according to the diffusion and accumulation characteristics of microleakage LPG, it can be inferred that if the leakage occurs in the lower cavity, the leaked LPG would accumulate in the cavity bottom and easily be ignited by sparks generated by the electrical appliances in the lower cavity to explode; however, if the leakage occurs in the upper cavity, then in addition to the ignition and explosion of the accumulated LPG at the bottom of the cavity, the accumulated LPG on the gas stove baffle will be ignited by a naked fire to explode as well (an explosion is more likely to occur when a naked fire is present).

Combined with the time required to reach the critical concentration of explosion at different leakage locations, it can be further concluded that for short-time leakage, if the leakage source is located in the lower cavity below the gas stove baffle, it may have a higher risk of combustion and explosion. For a sustained leakage over a certain period, the combustion and explosion risk will be much greater if the leakage source is located in the upper cavity above the gas stove baffle.

## 5. CONCLUSIONS

In this study, the diffusion and accumulation characteristics of microleakage LPG in an integrated stove were comprehensively analyzed, the differences of diffusion and accumulation characteristics at different leakage rates were compared, and the influence of leakage source location on diffusion and accumulation characteristics was also discussed. The conclusions of the research are as follows:

(1) Diffusion flow characteristics of microleakage LPG indicate that LPG will downward diffuse driven by gravity during the diffusion process. When the leakage source is located below the gas stove baffle, the diffused LPG exhibits accumulation characteristics in the cavity bottom, and the concentration of LPG at the bottom is approximately 1.0−1.3% higher than that at the top; when the leakage source is located above the gas stove baffle, the diffused LPG exhibits accumulation characteristics in the cavity bottom and on the gas stove baffle, and the concentration of LPG at the bottom is usually about 0.1−0.2% higher than that at the top. Because the accumulated LPG cannot escape from the confined space, so regardless of where the leakage source is located, the volume of the dangerous area rapidly changes with the continuous accumulation of LPG in the cavity, which occupies above 50% of the cavity volume.

(2) Spatial distribution characteristics of microleakage LPG indicate that LPG concentration distribution is extremely inhomogeneous. On the same longitudinal section, the concentration generally decreases with increasing height (except for the baffle); on the same cross section, the closer the location to the leakage source, the higher the concentration of accumulated LPG.

(3) The diffusion and accumulation characteristics of microleakage LPG at different leakage rates indicate that the diffusion and accumulation process of LPG under various leakage rates are highly similar, and the different leakage rates can only affect the concentration of LPG in the integrated stove, which means that the faster leakage rate can only accelerate the time to reach the critical concentration of explosion.

(4) The location of the leakage source is closely related to the diffusion and accumulation characteristics of the microleakage LPG. When the leakage source is located below the gas stove baffle, the time required for the concentration of LPG to accumulate in the integrated stove and reach the critical concentration of explosion is 2/3 of the time required when the leakage source is located above the gas stove baffle.

Based on the diffusion and accumulation characteristics of microleakage, when the leakage source is located below the gas stove baffle in the lower cavity, the bottom of the cavity is at explosion risk, and when the leakage source is located above the gas stove baffle in the upper cavity, the entire cavity is at explosion risk.

(5) According to the explosion risk analysis of microleakage LPG in the integrated stove, the relation between the explosion risk of different leakage source locations in the integrated stove and leakage time is obtained, which can be used to prevent combustion and explosion accidents in domestic gas appliances like integrated stoves.

## AUTHOR INFORMATION


### Corresponding Authors

**Kan Jin** − *College of Quality & Safety Engineering, China Jiliang University, Hangzhou, Zhejiang 310018, China; Zhejiang Institute of Product Quality and Safety Science, Hangzhou, Zhejiang 310018, China; Institute of Process Equipment, College of Energy Engineering, Zhejiang University, Hangzhou, Zhejiang 310027, China; State Key Laboratory Cultivation Base for Gas Geology and Gas Control, Henan Polytechnic University, Jiaozuo, Henan 454000, China;* orcid.org/0000-0002-7882-5710; Email: jinkan@outlook.com

**Dongmei Huang** − *College of Quality & Safety Engineering, China Jiliang University, Hangzhou, Zhejiang 310018, China;* orcid.org/0000-0003-3957-2156; Email: 20021567@163.com, dmhuang@cjlu.edu.cn

### Authors

**Gaofan Lin** − *College of Quality & Safety Engineering, China Jiliang University, Hangzhou, Zhejiang 310018, China*

**Qi Zhao** − *Zhejiang Institute of Product Quality and Safety Science, Hangzhou, Zhejiang 310018, China*

**Yajing Liu** − *Ministry of Production Safety Supervision, Zhejiang Provincial Energy Group Company Ltd., Hangzhou, Zhejiang 310007, China*

**Jia Qiu** − *Zhejiang Institute of Product Quality and Safety Science, Hangzhou, Zhejiang 310018, China*

**Yong Jiang** − *Zhejiang Institute of Product Quality and Safety Science, Hangzhou, Zhejiang 310018, China*

Complete contact information is available at:




https://doi.org/10.1021/acsomega.2c06715
ACS Omega 2023, 8, 1271−1281

https://pubs.acs.org/10.1021/acsomega.2c06715

### Notes

The authors declare no competing financial interest.

## ■ ACKNOWLEDGMENTS

The authors are grateful for the financial support from the National Natural Science Foundation of China (No. 51904282), the Natural Science Foundation of Zhejiang Province (LQ19E040004 and LGF21E040004), the State Key Laboratory Cultivation Base for Gas Geology and Gas Control, Henan Polytechnic University (WS2019B06), and the Natural Science Foundation of Liaoning Province (2020-KF-23-07).

## ■ REFERENCES

(1) Li, Y. B.; Wang, J. Technical analysis and development proposals of integrated cooker. *Shanxi Sci. Technol.* **2013**, *28*, 157−158.
(2) Ma, X. Y.; Lu, G. Y.; Wu, S. D. Study on fan performance optimization and supply air uniformity of integrated cooking appliance. *Electr. Appliances* **2022**, *07*, 30−34+38.
(3) China Household Electric Appliance Research Institute. 2021 annual report of Chinese household electric appliance industry. *Household Electr. Appliance* **2022**, *03*, 36−59.
(4) Sun, P. Customer Demand Analysis of Integrated Cooker Based on Kano Model: A Study of Entive in Thailand. MS Thesis, Siam University: Thailand, 2017.
(5) Peck, M. D.; Kruger, G. E.; Van Der Merwe, A. E.; Godakumbura, W.; Ahuja, R. B. Burns and fires from non-electric domestic appliances in low and middle income countries: Part I. The scope of the problem. *Burns* **2008**, *34*, 303−311.
(6) Tao, X. D.; Chen, Y. L.; Zhao, Q.; Jin, K. Law of micro-leakage diffusion of Liquefied Petroleum Gas in integrated stove. *Sci. Technol. Eng.* **2019**, *19*, 332−337.
(7) Luo, X. P. Family expenses of poor quality burns analysing making safe hidden trouble of cooking stove angary. *China Build. Mater. Sci. Technol.* **2014**, *23*, 177−179.
(8) Wang, D. Y.; Zhao, F. Y.; Wang, T. In *The Ultrasonic Characteristics Study of Weak Gas Leakage*, International Conference on Fluid Power and Mechatronics (FPM), Harbin, China, pp 681−685.
(9) Woodward, J. L. A model of indoor releases with recirculating ventilation. *Process Saf. Prog.* **2000**, *19*, 160−165.
(10) Furtaw, E. J., Jr.; Pandian, M. D.; Nelson, D. R.; Behar, J. V. Modeling indoor air concentrations near emission sources in imperfectly mixed rooms. *J. Air Waste Manage. Assoc.* **1996**, *46*, 861−868.
(11) Puttick, S. *Modelling the Dispersion of Spills in Buildings*, Symposium series. Hazards XXI; IChemE: 2009; pp 610−614.
(12) Cai, P.; Li, M. Z.; Liu, Z. Y.; Li, P. L.; Zhao, Y.; Zhou, Y. Experimental and numerical study of natural gas leakage and explosion characteristics. *ACS Omega* **2022**, *7*, 25278−25290.
(13) Brzezińska, D.; Dziubiński, M.; Markowski, A. S. Analyses of LPG dispersion during its accidental release in enclosed car parks. *Ecol. Chem. Eng.* **2017**, *24*, 249−261.
(14) Papanikolaou, E. A.; Venetsanos, A. G.; Heitsch, M.; Baraldi, D.; Huser, A.; Pujol, J.; Garcia, J.; Markatos, N. HySafe SBEP-V20: numerical studies of release experiments inside a naturally ventilated residential garage. *Int. J. Hydrogen Energy* **2010**, *35*, 4747−4757.
(15) Wu, Y.; Yu, E.; Xu, Y. *Simulation and Analysis of Indoor Gas Leakage*, Proceedings of IBPSA Conference, Beijing: China, 2007; pp 3−6.
(16) Dong, L. X.; Zuo, H. C.; Hu, L.; Yang, B.; Li, L. C.; Wu, L. Y. Simulation of heavy gas dispersion in a large indoor space using CFD model. *J. Loss Prev. Process Ind.* **2017**, *46*, 1−12.
(17) Ni, K.; Ma, Y. P. Simulation of LPG tank truck leakage and explosion accident based on CFD. *J. Phys.: Conf. Ser.* **2021**, *2003*, No. 012005.
(18) Ebrahimi-Moghadam, A.; Farzaneh-Gord, M.; Arabkoohsar, A.; Moghadam, A. J. CFD analysis of natural gas emission from damaged pipelines: Correlation development for leakage estimation. *J. Cleaner Prod.* **2018**, *199*, 257−271.
(19) Guo, Y. H. Diffusion Simulation of Indoor Flammable Gas Leakage and Analysis of Explosion Effects. MS Thesis, Chongqing University: China, 2011.
(20) Zhang, F. R.; Zhang, H.; Zhuang, C. L. CFD numerical simulation of dispersion law of indoor gas leakage based on weather conditions. *J. Cent. South Univ. Technol.* **2009**, *16*, 62−67.
(21) Wang, Y. The Diffusion Condition Simulation and Consequence Analysis of the Indoor Gas Leakage. MS Thesis, Chongqing University: China, 2007.
(22) Li, X. Q.; Wang, Z. T.; Tian, G. S.; Liu, J.; Li, D. S. Numerical analysis of the diffusion effects of combustible gas leak on the leak location. *Proc. Eng.* **2017**, *205*, 3678−3685.
(23) Tulach, A.; Mynarz, M.; Kozubkova, M. Study of distribution and quantification of flammable gas in confined space. *Appl. Mech. Mater.* **2014**, *638*−*640*, 2097−2100.
(24) Middha, P.; Hansen, O. R. CFD simulation study to investigate the risk from hydrogen vehicles in tunnels. *Int. J. Hydrogen Energy* **2009**, *34*, 5875−5886.
(25) Van Wingerden, K.; Wilkins, B.; Bakken, J.; Pedersen, G. The influence of water sprays on gas explosions. Part 2: mitigation. *J. Loss Prev. Process Ind.* **1995**, *8*, 61−70.
(26) Xin, B. Q.; Wan, L.; Dang, W. Y. Dynamic simulation and quantitative risk assessment of indoor heavy gas diffusion. *J. Phys.: Conf. Ser.* **2020**, *1549*, No. 042080.
(27) Fu, H.; Yang, L.; Liang, H. R.; Wang, S.; Ling, K. G. Diagnosis of the single leakage in the fluid pipeline through experimental study and CFD simulation. *J. Pet. Sci. Eng.* **2020**, *193*, No. 107437.
(28) Sun, H. C.; Hao, Y. Y.; Wang, L. N. Macroscopical contact pressure and microscopic leakage performance analysis of rubber seal considering thermal oxygen aging effect. *Proc. Inst. Mech. Eng., Part G* **2022**, *236*, 3129−3140.
(29) Sun, H. C.; Hao, Y. Y.; Song, T.; Wang, L. N. Research on micro-leakage performance of the rubber seal. *Proc. Inst. Mech. Eng., Part G* **2022**, *236*, 9061−9071.
(30) Liu, L. Z.; Zhu, Y. Z.; Yang, X. F. Experimental research on corrosion of DME/LPG mixture. *Gas Heat* **2013**, *33*, 34−37.
(31) Han, Y. F. Inner Mongolia region should strengthen the quality of Liquefied Petroleum Gas product regulation. *Inn. Mong. Petrochem. Ind.* **2015**, *41*, 53−54.
(32) Xu, X. D.; Wang, X. N.; Zhu, P.; Guo, P. J.; He, H. Experimental study on safety property of LPGDME rubber shim. *Chem. Eng. Mach.* **2012**, *39*, 578−581.
(33) Qi, R. F.; Ng, D.; Cormier, B. R.; Mannan, M. S. Numerical simulations of LNG vapor dispersion in Brayton Fire Training Field tests with ANSYS CFX. *J. Hazard. Mater.* **2010**, *183*, 51−61.
(34) Xing, J.; Liu, Z. Y.; Huang, P.; Feng, C. G.; Zhou, Y.; Zhang, D. P.; Wang, F. Experimental and numerical study of the dispersion of carbon dioxide plume. *J. Hazard. Mater.* **2013**, *256*−*257*, 40−48.
(35) Wang, J. J.; Cao, R.; Wang, Q. H.; Ma, M. H. Diffusion analysis of carbon dioxide released by egg respiration at different storage temperatures based on FLUENT. *Int. Food Res. J.* **2022**, *29*, 135−141.
(36) Liang, H.; Wang, T.; Luo, Z. M.; Wang, X. Q.; Kang, X. F.; Deng, J. Risk assessment of liquefied petroleum gas explosion in a limited space. *ACS Omega* **2021**, *6*, 24683−24692.
(37) China Municipal Engineering North China Design and Research Institute. *Safety Management Regulation of Gas-Burning Appliances for Domestic Use, GB 17905—2008*; Standards Press of China: Beijing, 2008.
(38) Bird, G. *Molecular gas dynamics NASA STI/Recon Technical Report A*, 1976; Vol. 76, p 40225.
(39) Zhu, H. Y. Experimental and Numerical Study of Leakage and Dispersion from Multi-source Gas. MS Thesis, University of Science and Technology of China: China, 2013.
(40) Zhu, D. Z. Example of simulating analysis on LNG leakage and dispersion. *Proc. Eng.* **2014**, *71*, 220−229.